A Comparison of Imaging Methodologies for 3D Tissue Engineering

LOUISE E. SMITH,[1] ROD SMALLWOOD,[2] AND SHEILA MACNEIL[1]*
[1]*Department of Engineering Materials, Kroto Research Institute, University of Sheffield, North Campus, Broad Lane, Sheffield S3 7HQ, United Kingdom*
[2]*Department of Computer Science, University of Sheffield, Regent Court, 211 Portobello, Sheffield S1 4DP, United Kingdom*

KEY WORDS confocal laser scanning microscopy; optical coherence tomography; electron microscopy

ABSTRACT Imaging of cells in two dimensions is routinely performed within cell biology and tissue engineering laboratories. When biology moves into three dimensions imaging becomes more challenging, especially when multiple cell types are used. This review compares imaging techniques used regularly in our laboratory in the culture of cells in both two and three dimensions. The techniques reviewed include phase contrast microscopy, fluorescent microscopy, confocal laser scanning microscopy, electron microscopy, and optical coherence tomography. We compare these techniques to the current "gold standard" for imaging three-dimensional tissue engineered constructs, histology. *Microsc. Res. Tech. 73:1123–1133, 2010.*

INTRODUCTION

Optical imaging of cells in two-dimensional (2D) tissue culture is routinely used in cell biology laboratories, but imaging of cells in three-dimensional (3D) tissue engineered constructs presents new challenges. This review compares the imaging methods currently used in the culture of cells in 2D and 3D (based largely on this laboratory's experience of these)—phase contrast microscopy, fluorescent microscopy, confocal laser scanning microscopy, electron microscopy, and optical coherence tomography (OCT). We contrast those methodologies that can only be done on fixed tissues at the end of experiments with those that can be undertaken in living tissues.

In brief, tissue engineered materials in the laboratory, are often a combination of more than one cell type in a 3D scaffold cultured for various periods of time from a few days through to several weeks. The challenge is to get information on the development of these tissues without the use of destructive histology that requires that one sacrifices samples to get this information. This latter approach currently necessitates setting up many replicates, some of which are stopped at different time intervals. This is clearly wasteful, and there is a need for noninvasive methodologies to provide information on the development of the tissues.

Table 1 summarizes the pros and cons of the various methodologies with respect to conventional 2D culturing and to use in 3D tissue engineering. Whilst Table 2 compares the depth of penetration and the resolution of the various tachniques.

PHASE CONTRAST MICROSCOPY

When viewing cells in two dimensions or in highly transparent, thin constructs, phase contrast microscopy is routinely used. Normal bright field microscopy renders most of the detail of living cells invisible as there is little or no contrast between the structures inside the cell. However, when light passes through a cell it will pass through many lipid membranes and will consequently be bent as the light passes through materials with varying refractive indices. Typical poor contrast images of human skin cells obtained by phase contrast microscopy are shown in Figure 1. Briefly structures with a high refractive index will bend oblique incidence light more than structures with a low refractive index. This also delays the light so that light that has passed through an interface between media of differing refractive indices will reach the observer slightly behind light that has not been bent. In addition to this light from most objects passes through all parts of the lens, the center, and the periphery. If the light passing through the periphery of the lens is retarded by half a wavelength ($\lambda/2$) and the light passing through the center of the lens not retarded then the light is out of phase by $\lambda/2$. When the image is brought into focus by the objective this is cancelled out and a reduction in the brightness of the image is observed. To use the phase contrast effect the path of the light must be aligned.

Although these images are easy to obtain and these are invaluable for the routine culture of cells, the level of contrast is low and hence the images difficult to record with a camera. (The cell culturer can get considerable information on the cell morphology by focusing of the objective through the plane of the cells so that it is easy to comment on the extent of cell spreading and adhesion for example but harder to get a good photographic record of this).

The contrast in these images can be increased by staining the cells with a compound such as MTT

*Correspondence to: Sheila MacNeil, Tissue Engineering Group, Kroto Research Institute, North Campus, University of Sheffield, Broad Lane, Sheffield S3 7HQ, United Kingdom. E-mail: s.macneil@sheffield.ac.uk

Received 11 January 2010; accepted in revised form 22 February 2010
DOI 10.1002/jemt.20859
Published online 27 April 2010 in Wiley Online Library (wileyonlinelibrary.com).

TABLE 1. A comparison of optical imaging techniques for cells in 2D and in 3D constructs

Methodology	Pros	Cons	Use in living or fixed cells	Use in 2D or 3D
Phase contrast microscopy	Readily available in cell culture labs. Easy to use No need to manipulate samples	Difficult to get high-resolution photographs. Resolution dependent upon the numerical aperture of the lens used and the camera.	Use in living or fixed cells. Can use metabolic indicators or other agent to improve contrast.	Works best in 2D. Can be used in very limited applications in 3D. Samples cannot be very thick and must be virtually transparent. A contrast agent helps.
Fluorescence microscopy	Use of a fluorophore provides better contrast	Fluorescence microscopes are expensive.	The majority of fluorophores work only in fixed permeablized tissues. However, recent developments such as cell tracker dyes and the use of transfected cells expressing fluorescent proteins are extremely valuable in opening these techniques out to non-destructive imaging.	Works best in 2D
	Can have general staining i.e. whole cells or more specific staining i.e. immunostaining	Cells / tissues have to be stained. Resolution dependent upon the numerical aperture of the lens used, and the camera.		Can be used in very limited applications in 3D. Samples cannot be very thick and must be virtually transparent.
Confocal laser scanning microscopy	Use of the confocal plane provides better resolution than normal fluorescence microscopy.	Equipment can be extremely expensive.	The majority of fluorophores work only in fixed permeablized tissues. However, recent developments such as cell tracker dyes and the use of transfected cells expressing fluorescent proteins are extremely valuable in opening these techniques out to non-destructive imaging.	Works in 2D or 3D.
	Can be used in reflectance mode so staining not always necessary.	Samples usually have to be stained.		Depth of penetration into 3D samples limited by the optics of the sample.
	Can collect high-resolution images from within tissues.	Depth of penetration limited by sample. Resolution dependent upon the numerical aperture of the lens used, the laser, and the camera.		
Histology	Provides detailed information about tissue architecture	Destructive: Samples have to be fixed, processed, embedded, sectioned, and stained.	Samples must be fixed.	3D slices through samples.
	Can stain for a range of cell and extracellular proteins using specific antibodies. Usually a routine procedure.	Processing can damage samples. Some of the solvents used can dissolve polymeric scaffolds. Resolution dependent on microscope and camera.		
Electron microscopy	Gives extremely high resolution images of samples.	Destructive.	Samples must be fixed.	Scanning electron microscopy provides en face images of the sample surface.
	Resolution of TEM can be better than 0.5 nm.	Extremely expensive equipment.		Transmission electron microscopy: samples must be extremely thin > 200 nm
	Resolution of SEM can be better than 10 nm.	Not suitable for all biological samples, imaged in a vacuum. Intensive sample preparation. Samples must be coated with a conductive coating.		

TABLE 2. Comparing the resolution and depth of penetration of the different optical imaging techniques

Technique	Wavelength used (nm)	Best resolution (nm)	Best depth of penetration (μm)
Light microscopy	380–760	200	Surface
Fluorescence microscopy	340–780	10	Surface
Confocal laser scanning microscopy	340–780	10 (800 nm in *Z* direction)	300
Optical coherence tomography	800–1,300	500	1,000
Scanning electron microscopy	N/A	10	Surface
Transmission electron microscopy	N/A	0.5	Surface

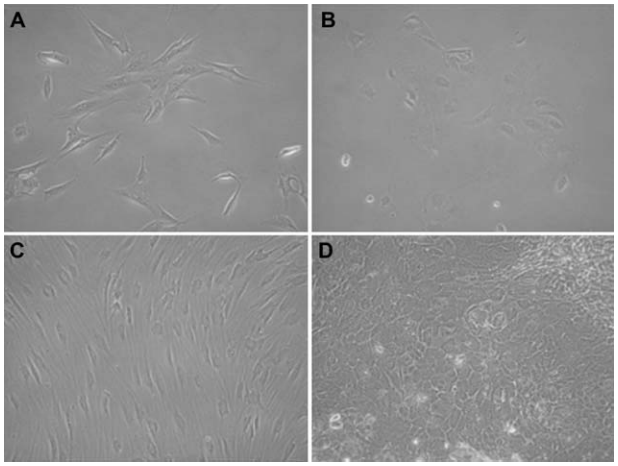

Fig. 1. Photomicrographs of human cells in 2D monolayer culture. (**A**) Melanocytes, (**B**) endothelial cells, (**C**) fibroblasts, and (**D**) keratinocytes.

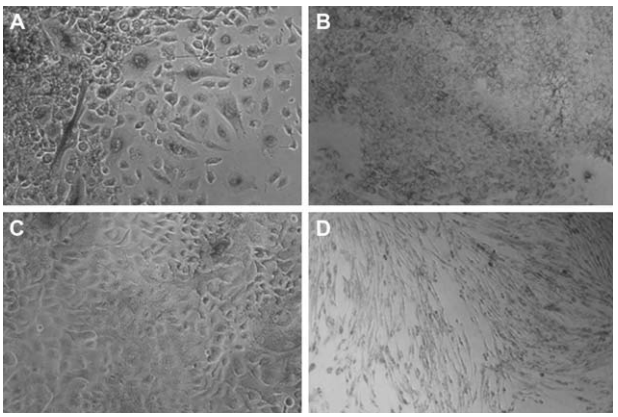

Fig. 2. Photomicrographs of human cells in 2D monolayer culture on tissue culture polystyrene. (**A**) Human corneal epithelial cell line, (**B**) HaCaT cell line, (**C**) keratinocytes, and (**D**) fibroblasts. All cells have been stained with MTT for 40 min prior to photographing.

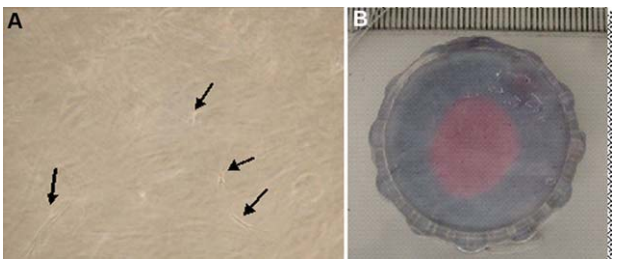

Fig. 3. (**A**) Phase contrast image of fibroblasts growing in a 2.7 mg/ml collagen gel. Arrows indicate location of fibroblasts. Note that not all of the cells identified are in focus; the cells can be seen coming in and out of focus when one manually adjusts the focal depth. (**B**) Photograph of tissue engineered skin stained with Alamar Blue. The pink circle in the center indicates the location of the keratinocytes cultured on this human acellular de-epidermised dermis (as detailed in Bullock et al., 2007) but individual cells cannot be seen (Image courtesy of Dr. A. Bullock).

(3-(4,5-Dimethyl-2-thiazolyl)-2,5-diphenyltetrazolium bromide) shown in Figure 2, which is often used to measure cell viability. The MTT is reduced to an insoluble purple colored formazan product inside viable cells. This remains inside the cell until it is eluted when the cell membrane is dissolved. In broad terms, the more dye produced the greater the metabolic activity of the cells. However, prior to elution of the purple product (usually after 30–45 min or so) the stained cells can be photographed using the phase contrast microscope.

This metabolic indicator while providing good contrast is toxic to the cells and so is only used at the end of the experiment. Similarly if cells are grown in a 3D construct (e.g., a collagen gel or a hydrogel through which light can penetrate) then phase contrast microscopy can also be used to image cells but it is very difficult to identify unstained cells in 3D as shown in Figure 3. Again addition of an agent to provide visible contrast can help, as with 2D culture the metabolic indicator MTT provides good contrast but kills the cells. An alternative indicator Alamar blue is converted by living cells from an initial blue to a pink end-point, which is nontoxic to cells. This means cells can continue to be cultured without loss of viability. Unfortunately this pink end point does not provide as strong a visual contrast for staining as the MTT metabolic assay (Fig. 3B).

FLUORESCENCE MICROSCOPY

Fluorescence microscopy utilizes the principles of fluorescence to visualize cells. Fluorescence is a three-stage process of excitation, nonradiative excited state transitions, and fluorescence emission (White and Errington, 2005). Generally, fluorescent molecules are polyaromatic hydrocarbons or heterocycles and are called fluorophores or fluorescent dyes. Basically, when a fluorophore absorbs a photon of light the fluorophore is excited from the ground state. The nonradiative excited state transitions represent important routes to energy states from which energy may eventually be lost from the molecule. The final stage of fluorescence emission is when a photon of energy is lost from the molecule returning the fluorophore to its ground state. Because of the energy lost during the nonradiative excited state transitions this photon has a lower energy, and therefore longer wavelength, than the one

that was absorbed when the molecule became excited. This difference in wavelength is called the Stokes shift.

While good-quality images and photographs can be taken the majority of fluorescence techniques have until comparatively recently been designed to be done on fixed and permeabilized (and hence dead) cells. There is an extensive range of antibodies linked to fluorescent dyes which give excellent quality images in 2D cultures of fixed cells as shown in Figure 4.

With systems such as ImageXpress by AXON (Axon Instruments/Molecular Devices, Union City, CA) fluorescence microscopy can be used to image into 3D constructs. These systems are good for finding the general location and number of cells; however, the image quality deteriorates with depth. The samples to be imaged have to be thin and virtually transparent. Fibrin gels or electrospun scaffolds are ideal scaffold materials for this. The images obtained are usually en face slices through the sample. This means that 3D experiments with a fluorescence microscopy end point have to be carefully thought out to increase the chances of getting good images. Sun et al. (2006) developed thin chambers containing fibrin clots to allow the interactions between fibroblasts and keratinocytes to be studied. These cultures could be followed using a fluorescence microscope when the chambers were placed on their side allowing slices through the fibrin gel to be imaged. This gave information on what was occurring inside the gel with an en face image as shown in Figure 5. These images were collected by staining cells with a CellTracker fluorescent dye, which enters live cells and can be used to visualize them for several days without damage to the cells.

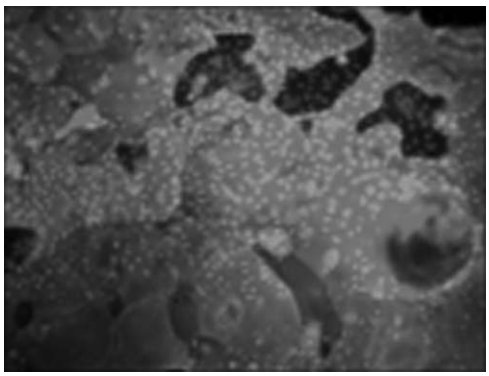

Fig. 4. A near confluent 2D culture of keratinocytes cocultured on a feeder layer of terminally irradiated murine fibroblasts stained with DAPI (blue) and a FITC (green) conjugated antibody, anti-involucrin, taken using a Leica epifluorescent microscope. DAPI indicates the nuclei of all cells and Involucrin is expressed only by keratinocytes.

CONFOCAL LASER SCANNING AND MULTIPHOTON MICROSCOPY

Generally, in vitro confocal microscopy is used in fluorescence mode. Confocal microscopes consist of a light source, a condenser, an objective lens, and a detector. The basic premise of confocal microscopy is the selective collection of light from in focus planes in the specimen. Depending on the lenses used this can be within a tissue, construct, or individual cells. With the use of a low-power near-infrared laser, a beam of light is focused tightly on a specific point in the sample. Light scattered or reflected from this illuminated point is collected through a pinhole-sized aperture by a detector. The light source, illuminated point, and detector aperture are in optically conjugated focal planes (i.e., confocal planes). This allows for the collection of light from the single in focus plane and the rejection of light from all out of focus planes (Nehal et al., 2008).

To image cells using fluorescent microscopy and fluorescence mode confocal microscopy, cells need to be stained with either generic compounds designed for live cell imaging such as CellTracker™ (Rimmer et al., 2007) or CelLuminate™ (Lomas et al., 2008), quantum dots (Chen et al., 2008; Smith et al., 2006) or with fluorescent dyes that are essentially toxic to cells or require cells to be leaky or permeabilized to enter the cells or with fluorophore-linked antibodies that again require cells to be fixed and permeabilized for their entry into the cells.

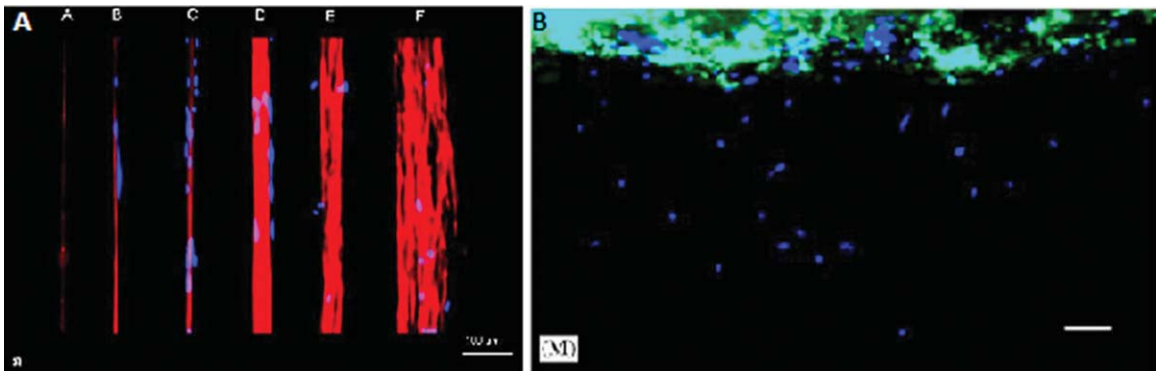

Fig. 5. Fluorescent micrographs taken using ImageXpress from AXON of slices through 3D cultures. (**A**) Fluorescent micrographs of human dermal fibroblasts cultured on electrospun aligned PLLA fibers of different diameters for 2 weeks. Each symbol represents a single fiber of increasing dimensions with cells cultured on them for 2 weeks. Scale bars are 100 μm. The red staining of the fibers is rhodamine added to the polymer solution during the elctrospinning process. The blue staining is DAPI staining of nuclei following permeabilization of the cells. Image from Sun et al. (2007a). (**B**) Cell Tracker™ Green stained keratinocytes and normal human dermal fibroblasts cocultured on fibrin gel in chamber II, retrospectively labeling nuclei with DAPI after experimentation. Image from Sun et al. (2006). [Color figure can be viewed in the online issue, which is available at wileyonlinelibrary.com.]

For example, DAPI (4′,6-diamidino-2-phenylindole) and propidium iodide are fluorescent stains that bind strongly to DNA and phalloidin conjugates bind strongly to F-actin. These stains can be used either individually or in combination. To stain cells for cytokeratins or involucrin as in Figure 4 then antibodies to keratins are used linked to fluorescent indicators.

In contrast, CellTracker™ and CelLuminate™ can be used to image live cells over a prolonged period of time. We have used these stains to visualize live cells over a period of up to 7 days for the CellTracker™ and 15 days for the CelLuminate™.

TABLE 3. Overview of excitation, emission, and fluorescence maxima of a variety of fluorescent biomolecules Data from Konig and Riemann (2003) and Schenke-Layland (2008)

Fluorophore	Excitation wavelength λ_{ex} (nm)	Emission wavelength λ_{em} (nm)	Fluorescence lifetime τ (ns)
Keratin		525	
NAD(P)H	340	450–470	0.3–0.6
Flavins	370, 450	530	5.2
Melanin	UV/VIS	440, 520, 575	0.2/1.9/7.9
Elastin	300–340	420–460	0.2–0.4/0.4–2.5
Collagen	300–340	420–460	0.2–0.4/0.4–2.5
SHG	720–960	360–480	0
Lipofuscin	UV/VIS	570–590	Multiexponential
Protoporphyrin IX (PPIX)	405, 630	635, 710	11

The advent of fluorescent dyes that can enter cells allowing the cells to be imaged nondestructively is extremely valuable for tissue engineering. However, where tissues contain more than one cell type then it is necessary to separately label the different cells before putting them into the construct. The next challenge is that as the cells divide they will dilute the fluorescent dye and also as the cells are imaged progressively so there is photobleaching of the dyes. A final challenge is that many tissue-engineered constructs are based on collagen scaffolds, and these develop a bright autofluorescence that extends over a broad range of wavelengths. Hence, in practice it can be very difficult to find a combination of fluorophores capable of distinguishing two cell populations from each other against a background with a high level of autofluorescence. The autofluorescent properties of various extracellular matrix proteins while often hindering the imaging of cells can be useful in their own right, e.g., it is possible to image collagen deposition onto scaffolds using nothing but the intrinsic optic properties of the molecules and second harmonic generation (Sun et al., 2008). An overview of the excitation and emission wavelengths for a number of biomolecules is given in Table 3.

While collagen in itself is extremely autofluorescent, many polymeric scaffolds are also fluorescent, as shown in Figure 6 below. In Figure 7, it is just about possible to distinguish the human dermal fibroblasts (HDFs) from the viscose rayon scaffold that they are

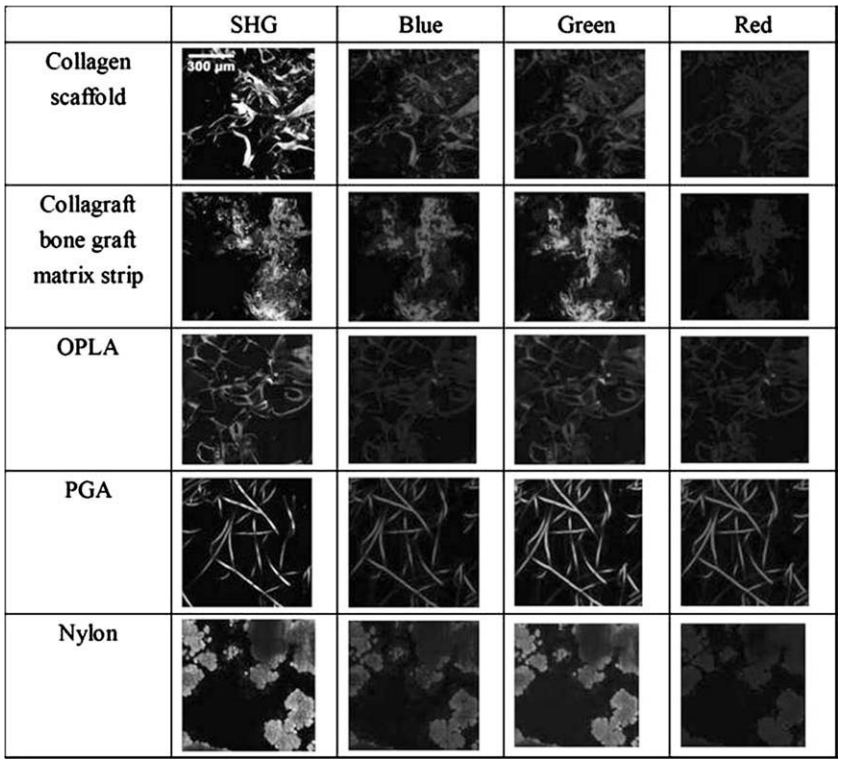

Fig. 6. Multiphoton autofluorescence and SHG imaging of the tissue engineering scaffolds of collagen, collagraft (Collagen, hydroxyapatite and tricalcium phosphate composite), open-cell poly(lactic acid) (OPLA), poly(glycolic acid) (PGA), and nylon. The autofluorescence is separated into the blue (435–485 nm), green (500–550 nm), and red (550–630 nm) channels. Image from Sun et al. (2008)

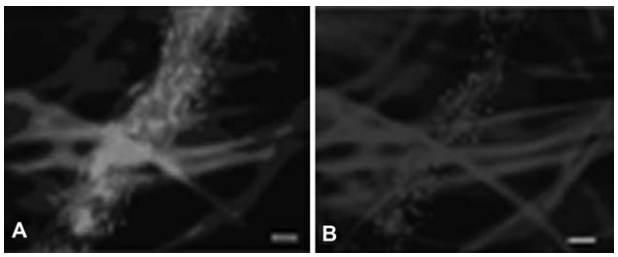

Fig. 7. Transfection of HDFs in 3D electrospun (nonwoven viscose rayon bonded with styrene butadiene copolymer) scaffolds. (**A**) HDFs were transfected in 3D electrospun viscose rayon scaffolds using a constitutively active EGFP plasmid to determine transfection efficiency. (**B**) The total number of cells was measured by counting nuclei using DAPI fluorescence labeling, enabling a percentage transfection efficiency of 40–80% to be calculated. Autofluorescence of scaffold fibers was observed at the excitation wavelengths used (λ_{ex} = 495 nm for EGFP detection and λ_{ex} = 358 nm for DAPI detection) enabling identification. Bar = 50 μm. (Canton et al., 2007).

growing on. The cells have been transiently transfected with an enhanced green fluorescent protein (EGFP) plasmid. The scaffold itself fluoresces at the wavelengths used to image both the cells and DAPI stained nuclei (λ_{ex} = 495 nm for EGFP detection and λ_{ex} = 358 nm for DAPI detection). Many polymers used as tissue engineering scaffolds are intrinsically autofluorescent.

Alternatively the cells can be genetically modified so that they produce a fluorescent protein, i.e., green fluorescent protein (GFP) as in Figure 7 above or red fluorescent protein (RFP). These proteins (derived from jellyfish) are not naturally found in mammalian cells but can be introduced genetically, usually downstream of a promoter of interest so that when this promoter is activated the cells express the fluorescent protein. To introduce the protein into the cells they have to be transfected. Transfection is the introduction of foreign DNA into a eukaryotic cell using a vector. Transfection can be accomplished using a variety of methods, dextran mediated transfection, lipofectin (Feril et al., 2005). and calcium phosphate (Dimond, 2007) mediated transfection are commonly used. Other techniques include electroporation, nucleofection (Hamm et al., 2002; Martinet et al., 2003), sonication (Feril et al., 2005), micro-injection (Kopchick and Stacey, 1984), and the use of polymersomes (Lomas et al., 2007).

Not all cells are readily transfected. Fibroblasts are relatively straightforward. Other primary cells such as epithelial cells are more challenging and one cannot assume that the transfected cell is entirely normal. This has to be proven. Further most transfections are transient transfections. Thus, transfection of cells can be useful but this methodology is not without problems.

Examples of confocal images using CellTracker and transfection are shown in Figure 8. Here A375-SM melanoma cells have been stained with the rhodamine based CelLuminate™, and the H1299 lung carcinoma cells have been stably transfected with plasmid DNA to produce a green fluorescent protein. In contrast, in picture C specific staining is shown. Rat schwannoma (RN22) cells have been fixed and stained with phalloidin-FITC and DAPI. The phalloidin-FITC has stained the F-actin in the cell cytoskeleton while the DAPI has bound to the nucleic acids inside the cell nucleus.

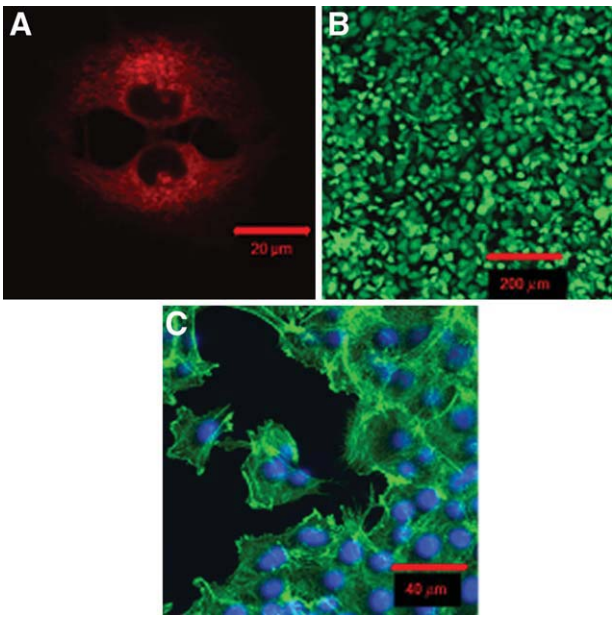

Fig. 8. CLSM images of monolayer cultures of cells. (**A**–**C**) cultured on tissue culture polystyrene, (**D**) cultured on glass. (A) A375-SM melanoma cells grown on tissue culture polystyrene and stained with CelLuminate™. (B) H1299-EGFP human lung carcinoma cell line stably transfected with pEGFP (Image courtesy of Dr. Irene Cantón). (C) RN22 rat schwannoma cells fixed with 10% buffered formalin and stained with Phalloidin-FITC to stain the cytoskeleton (green) and DAPI to stain the nuclei (blue) (Image courtesy of Miss Celia Murray-Dunning). [Color figure can be viewed in the online issue, which is available at wileyonlinelibrary.com.]

Confocal microscopy has better resolution at depth than conventional fluorescence microscopy. We have successfully used confocal microscopy (Zeiss LSM 510) to image cells stained with CellTracker Red™ growing in polymeric scaffolds that are up to 1 mm thick. It has also been possible to monitor the penetration of fluorescently labeled polymeric vesicles through tissue engineered skin, as shown in Figure 9.

Thus confocal fluorescence microscopy, which allows one a certain depth of imaging plus the excellent quality of imaging of a fluorescence microscope, is currently the leading edge imaging technology for viewing cells in 3D structures. However, the limitations on this is that it requires light penetration through the structure, so penetration into more dense scaffolds is very limited and there is a finite length of depth penetration that is generally of the order of 200–300 μm.

As previously mentioned, fluorescent dyes capable of entering living cells have greatly extended the range of experiments that can now be undertaken nondestructively. Further progress is on the horizon. Thus, polymersomes delivering fluorescently tagged antibodies into cells have been developed in the Battaglia group and allow imaging of specific features within cells nondestructively (Lomas et al., 2008).

OPTICAL COHERENCE TOMOGRAPHY

OCT has been used clinically in dermatology and in ocular applications for a while. While in vivo imaging of skin is performed routinely, imaging of ex vivo samples has proved troublesome with samples losing con-

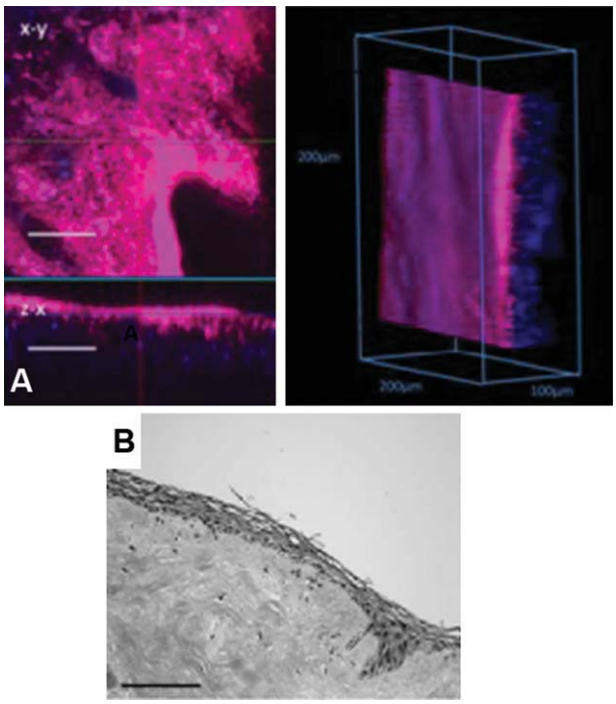

Fig. 9. (**A**) CLSM image of a tissue engineered oral mucosa model exposed to rhodamine-labeled $PMPC_{25}$-$PDPA_{70}$ for 48 h. Images on the left show *x-y* and *x-z* sections. The image on the right is a 3D projection of this model. Scale bar 50 μm. (**B**) Hematoxylin and eosin stained section of tissue engineered oral mucosa cultured for 10 days at air liquid interface. Scale bar 200 μm. Images from Hearnden et al. (2009). [Color figure can be viewed in the online issue, which is available at wileyonlinelibrary.com.]

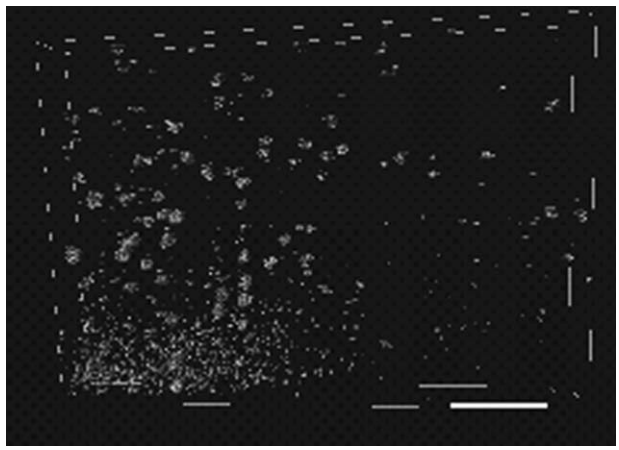

Fig. 10. OCT of cell migration. 3-D OCT images demonstrate the migration of macrophages through matrigel coated porous membranes. Scale bar 100 μm. Image from Tan et al. (2006).

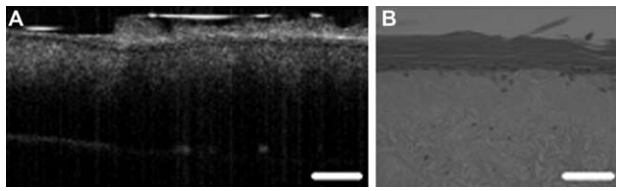

Fig. 11. OCT images of tissue engineered skin based on de-epithelialized acellular dermis. (**A**) Image taken using a Thorlabs OCS1300SS Swept Source OCT system. (**B**) H&E stained section through the tissue engineered skin. Scale bar = 250 μm. Image A courtesy of Dr. Marco Bonesi.

trast almost immediately upon excision from the tissue (Du et al., 2001; Hsiung et al., 2005). More recently, OCT has been applied to tissue engineering. It has been used to characterize the architecture of porous poly(lactide) and fibrous chitosan scaffolds (Yang et al., 2006a, 2007). In both cases it was possible to visualize the internal structure of the scaffolds, pore size, channel diameter, and fiber diameter could be calculated without destroying the scaffold. The fibrous chitosan scaffolds were used inside a perfusion bioreactor to support the growth of tissue engineered tendon. OCT was used to monitor the growth of the tendon inside the bioreactor. It was possible to see tissue development over time as indicated by an increase in light backscattered to the detector from the construct (Bagnaninchi et al., 2007a,b). OCT has also been used to monitor the invasion of cells into collagen gels. Unfortunately, the resolution of this OCT system is such that individual cells cannot be visualized (Yang et al., 2006b). Conversely, the group of Stephen Boppart have reported the use of OCT to noninvasively monitor cell migration in to a 3D model. The system used in this study used a Nd:YVO_4-pumped Ti-Saph laser that allowed a resolution of 10 μm to be obtained as shown in Figure 10 (Boppart et al., 2005; Tan et al., 2005, 2006). In these studies, a bench-top fiber-based time-domain OCT system was used with a 1,300 nm superluminescent diode (SLED), which had a bandwidth of 52 nm. An OCT system centered at 842 nm has also been used to image tissue engineered atherolike vascular tissue constructs and to identify smooth muscle cell rich areas and differentiate these from macrophage rich areas. However, the OCT system was unable to identify the exact location of lipids that had been loaded into the system (Levitz et al., 2007). OCT has also been used to monitor the calcification of gelatin sheets and sponges soaking in simulated body fluid. The increase in the scattered light corresponded to an increase in calcification. In some cases, the light was completely backscattered indicating that particles had been formed that were larger than the resolution of the system and that these were preventing the light from penetrating into the sample (Ishii et al., 2007).

Figure 11 shows images of tissue engineered skin based on a dermal matrix of deepithelialized acellular human dermis to which cultured keratinocytes and fibroblasts have been added to reconstitute tissue engineered skin (Fig. 11A). Figure 11B shows an OCT image of this using a Thorlabs OCS1300SS Swept Source OCT system. This clearly shows depth penetration but with very little detail. Images of reconstructed skin where the dermal component is a fibroblast-populated amorphous collagen gel (Spoler et al., 2006; Yeh et al., 2004) have also been achieved.

Despite its lack of detail, OCT is emerging as a new noninvasive methodology for following tissue engineering which can deliver depth of resolution. It is also a technique that is under further development at pres-

ent; at present, it currently offers unparalleled depth penetration and is totally noninvasive, allowing imaging of 3D tissues as they develop with time without the need for destructive histology. If further developments can yield increased spatial resolution to go alongside the depth of resolution, then OCT will join the armoury of routine techniques for tissue engineers.

HISTOLOGY

Histology is the gold standard by which most tissue engineered constructs are evaluated. The unfortunate consequence of this is that it involves the sacrifice of the sample. Therefore, when using histology to monitor construct development a large number of samples are needed. Conventional histology involves fixing the sample, the sample is then dehydrated, and embedded in paraffin wax. Once sectioned and mounted on a slide the sample can be stained as shown in Figure 12, some common stains are listed in Table 4 below and examples of H&E stained sections are shown in Figure 12.

If a sample cannot be processed for histology using paraffin embedding, because for example the solvents used will dissolve the scaffold supporting the tissue engineered construct, it is still possible to image the sample using cryo-sectioning. Samples, once fixed, can be embedded in a tissue-freezing medium such as OCT from TissueTEK or a solution of poly(ethylene glycol) in water. These samples are then frozen in a cryo-mold in liquid nitrogen and sectioned using a cryostat. This procedure is especially useful for immunohistochemistry samples, see Figure 13, where specific antibodies have been used to identify cell types (keratinocytes as in Fig. 13B) or extracellular matrix proteins (collagen IV as in Figs. 13B and 13C) and samples where the solvents and conditions used to process the sample for paraffin embedding, ethanol, xylene, paraffin, high temperatures, could damage the sample.

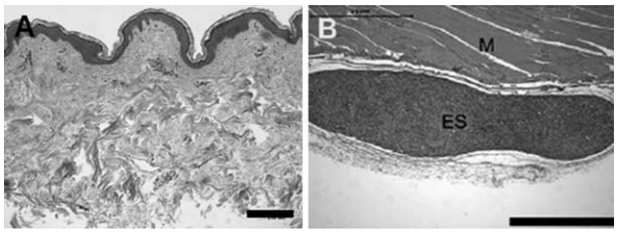

Fig. 12. (**A**) H&E staining of tissue engineered skin based on deepithelialized acellular dermis. (**B**) Light microscope H&E image of PLLA electrospun scaffold following implantation into the flank of adult male Wistar rat at 5 months. Implanted scaffold has been labeled as (ES), with underlying muscle (M) and skin (S). Scale bar A = 250 μm, B = 1 mm. Image B from Blackwood et al. (2008).

ELECTRON MICROSCOPY

Electron microscopy is increasingly being used in tissue engineering and in the evaluation of biomaterials. Once again, this is a terminal technique as the samples have to be frozen and fixed. The samples are then dehydrated, freeze dried, bisected and mounted, sputter coated with gold, placed in a vacuum and bombarded by high-energy electrons. Despite this, electron microscopy, particularly scanning electron microscopy (SEM) can provide vital information. Depending on the instrument, scanning electron microscopes have a resolution of between 1 and 5 nm with a transmission electron microscope providing a resolution of down to 0.2 nm. However the fixing process required for biological samples gives an effective resolution of 2 nm (Studer et al., 2008). Figure 14 shows SEM images of various polymers and cells attached to these polymers. Figure 14A shows the structure of an electrospun PLLA-PLGA scaffold and allows the fiber diameter to be measured. Human dermal fibroblasts and keratinocytes can be grown on this scaffold and self-organize to produce an epidermal layer and a dermal layer with the fibroblasts growing on and around the scaffold, Figure 14B.

Transmission electron microscopy (TEM) can also be used to image in tissue engineering. It is not used to visualize cells as a whole, but more to look inside cells. This is because to get a good TEM image the sample has to be very thin at the region of interest, about 1,000 Å. This minimizes the number of atoms in the path of the electron beam and allows for a clearer image. Figure 15 shows TEM images of tissue engineered oral mucosa. The TEM images show the ultrastructural organization

TABLE 4. List of some commonly used histological stains

Stain	Description
Hematoxylin and Eosin (H&E)	This is a standard histology stain. Hematoxylin binds to acidic structures (i.e. nucleic acids) staining them blue/purple. Eosin is an acid aniline dye which binds to basic or negatively charged structures (i.e. cytoplasm, muscle, connective tissue, red blood cells, and decalcified bone matrix) and stains them pink/orange/red.
Alizarin Red S	Stains calcium in tissue sections red.
Alkaline Phosphatase	Stains areas of alkaline phosphatase activity red and cell nuclei blue. Can be used to determine if mesenchymal stem cells are differentiating to an osteoblast lineage.
Fontana-Masson	This silver based stains melanin black, cell nucleus pink/red and cytoplasm light pink.
Masson Trichrome	This uses three dyes light green, iron hematoxylin and acid fuchsin to stain connective tissue. Collagen, mucus, ground substance will be green (collagen very green). Muscle and keratin stain red, cytoplasm pink/red, and cell nuclei stain black.
Oil Red O	Stains for lipids. Lipids stain red, cell nuclei stain blue/black.
Papanicolaou (PAP) stain	Five stains in three solutions. Hematoxylin stains cell nuclei blue/purple. Orange G (OG-5, OG-6, or OG-8) stains keratin orange. Eosin Azure (EA-36, EA-50, EA-65) stains cytoplasm, collagen, muscle fibers, and mucus a yellow/green.
Periodic Acid-Schiff	Glycogen, mucin, mucoprotein and glycoproteins stain magenta. Cell nuclei stain blue and collagen stains pink.
Sirius Red	Stains collagen red
Van Gieson	Used to differentiate between collagen and smooth muscle. Cytoplasm, fibrin, and muscle stain brown/yellow, collagen red, and cartilage pink.

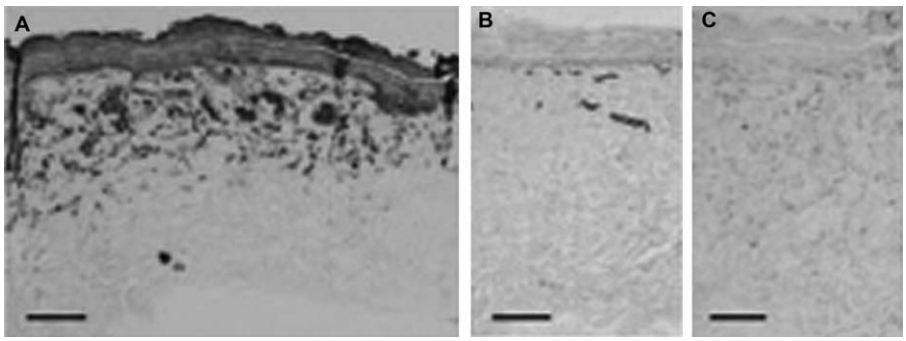

Fig. 13. Effect of estrone and estradiol on tissue engineered skin. (**A**) A dense dermal infiltrate is seen on culture with estrone (1 nM). This dermal infiltrate stains positive for pancytokeratin indicating these are keratinocytes. (**B**) Collagen IV staining reveals preservation of the basement membrane in control TE skin, and (**C**) loss of basement membrane during culture with 1 nM estrone. Scale bar = 100 μm. Image from Harrison et al. (2006).

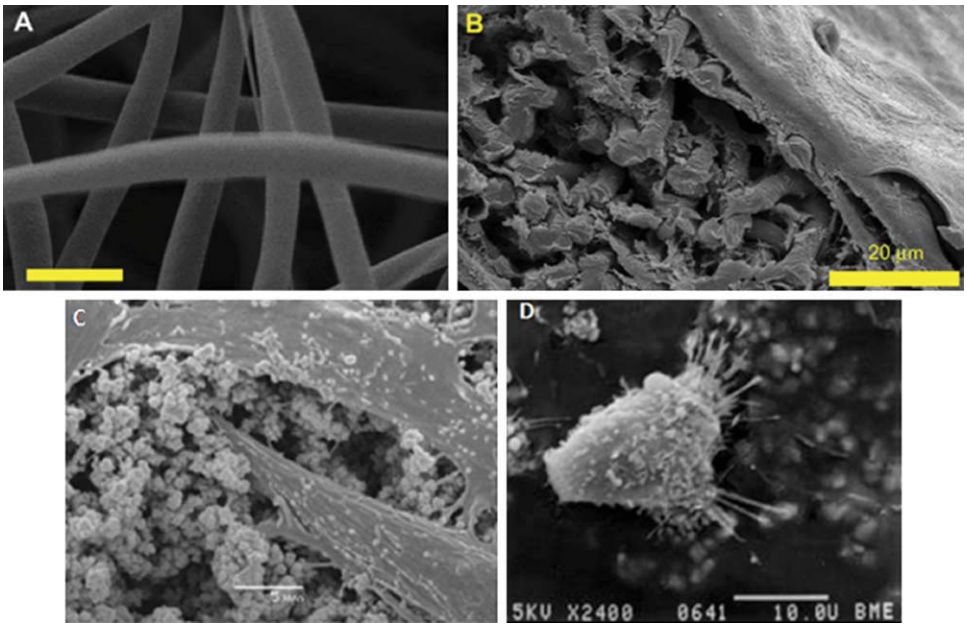

Fig. 14. SEM images of (**A**) electrospun PLLA:PLGA 85:15 scaffolds, (**B**) SEM micrograph of keratinocytes and fibroblasts cocultured on a PLLA:PLGA 75:25 scaffold for 7 days (Blackwood et al., 2008), (**C**) SEM micrograph of human dermal fibroblasts cultured on GMMA polymer for 4 days (Sun et al., 2007b), (**D**) SEM of human osteoblast-like (HOB) cell cultured on hydroxyapatite (HA) filled poly(methylmethacrylate) (PMMA). The cell has normal osteoblast morphology. The cellular processes can be seen to extend, and preferentially attach, to HA crystals exposed at the cement surface (Dalby et al., 1999). [Color figure can be viewed in the online issue, which is available at wileyonlinelibrary.com.]

of the tissue, specifically the epithelium, lamina propria, and basement membrane. The TEM images were also able to show newly synthesized collagen with the striations of the collagen fibrils becoming visible at higher magnifications (Kinikoglu et al., 2009).

CONCLUSION

Imaging is vital when monitoring the development of cells and tissues, whether it is to check for infection or the degree of confluency or to determine the endpoint of an experiment. Unfortunately, until very recently most imaging techniques that allowed one to collect good images for publication required a degree of sample preparation which involved terminating the experiments. Thus, the majority of fluorescent tags are designed to work with fixed and permeablized cells. Conventional histology similarly requires fixed tissues as does the electron microscopy. All of these are capable of delivering very good-quality images but require the sacrifice of many 3D cultures of cells.

The ability to noninvasively monitor cell and tissue development is crucial for 3D tissue engineering. Phase contrast microscopy allows the nondestructive monitoring of monolayers of cells to be monitored but struggles to clearly identify cells even within thin transparent collagen gels. OCT allows noninvasive visualization of tissues with a depth of penetration dependent on the wavelength of the light used.

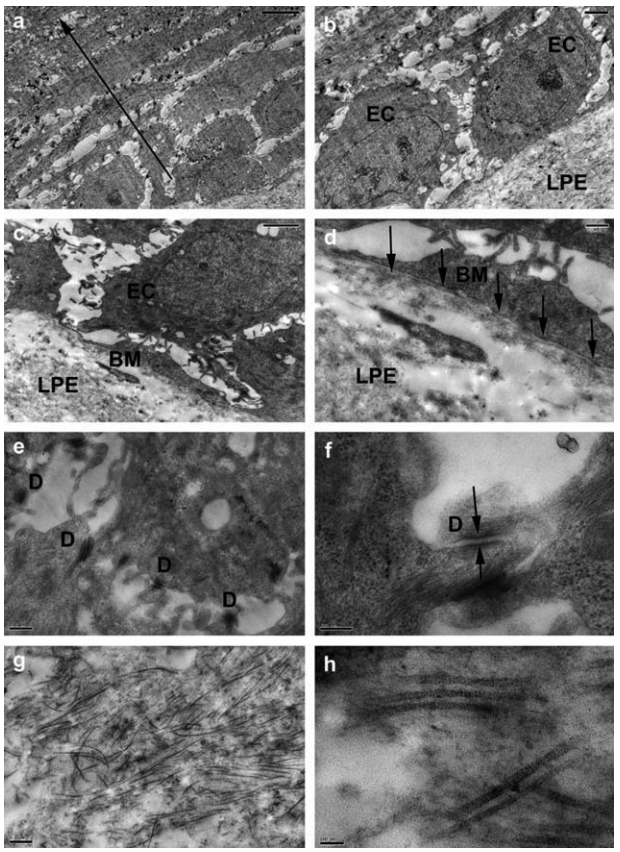

Fig. 15. Ultrastructural analysis of the oral mucosal equivalent by transmission electron microscopy (**A**) different cell layers and differentiation in the epithelium, epithelial cells become flattened as they move from the basal up to superficial layer (arrow) (bar = 5 μm), (**B**) two adjacent basal epithelial cells (ECs) residing on the lamina propria equivalent (LPE) (bar = 2 μm) (**C**) basement membrane (BM) formed between the LPE and the epithelium (bar = 2 μm), (**D**) the continuous and well-organized BM at higher magnification anchoring the epithelium firmly to the LPE (bar = 0.5 μm), (**E**) numerous desmosomes were detected between adjacent epithelial cells (bar = 0.5 μm), (**F**) a desmosome at higher magnification (bar = 200 nm), (**G**) newly synthesized collagen I fibrils in the LPE (bar = 0.5 μm), and (**H**) collagen fibril striations visible at higher magnification (bar = 100 nm). Image from Kinikoglu et al. (2009).

However, currently OCT does not give cellular resolution that is at all comparable with other techniques, but this may be possible in the future with better light sources. The imaging technique used will ultimately depend on the resolution and magnification required.

For the majority of experimentation in tissue engineering currently the ideal situation is some level of noninvasive imaging as the 3D constructs are grown followed by destructive imaging when the information obtained from OCT suggests the experiment is complete. Thus, OCT currently offers a methodology for nondestructive imaging of constructs but without good resolution. The latter is currently gained by subsequently imaging the tissue. using confocal microscopy, conventional histology or electron microscopy, all of which are possible once the tissue is sacrificed.

In conclusion, OCT fills a gap in the techniques available for tissue engineers and it also has the potential to be significantly improved. The use of OCT also does not limit one's options to subsequently using any other technique to gain information on the tissue engineered construct and our prediction is that this will become much more routine technology for imaging of developing tissue engineered constructs.

REFERENCES

Bagnaninchi PO, El Haj A, Yang Y. 2007a. Continuous monitoring of tissue growth inside a perfusion bioreactor by optical coherence tomography. Prog Biomed Opt Imaging: Proc of SPIE 6439:6439C.

Bagnaninchi PO, Yang Y, Zghoul N, Maffulli N, Wang RK, Haj AJ. 2007b. Chitosan microchannel scaffolds for tendon tissue engineering characterized using optical coherence tomography. Tissue Eng 13:323–331.

Blackwood KA, McKean R, Canton I, Freeman CO, Franklin KL, Cole D, Brook I, Farthing P, Rimmer S, Haycock JW, Ryan AJ, MacNeil S. 2008. Development of biodegradable electrospun scaffolds for dermal replacement. Biomaterials 29:3091–3104.

Boppart SA, Tan W, Ko HJ, Vinegoni C. 2005. Optical coherence tomography of cell dynamics in three-dimensional engineered tissues. Prog Biomed Opt Imaging: Proc of SPIE 5861:58610Z.

Bullock AJ, Barker AT, Coulton L, Macneil S. 2007. The effect of induced biphasic pulsed currents on re-epithelialization of a novel wound healing model. Bioelectromagnetics 28:31–41.

Canton I, Sarwar U, Kemp EH, Ryan AJ, Macneil S, Haycock JW. 2007. Real-time detection of stress in 3D tissue-engineered constructs using NF-kB activation in transiently transfected human dermal fibroblast cells. Tissue Eng 13:1013–1024.

Chen L-D, Liu J, Yu X-F, He M, Pei X-F, Tang Z-Y, Wang Q-Q, Pang D-W, Li Y. 2008. The biocompatibility of quantum dot probes used for the targeted imaging of hepatocellular carcinoma metastasis. Biomaterials 29:4170–4176.

Dalby MJ, Di Silvio L, Harper EJ, Bonfield W. 1999. In vitro evaluation of a new polymethylmethacrylate cement reinforced with hydroxyapatite. J Mater Sci Mater Med 10:793–796.

Dimond PF. 2007. In vitro nucleic acid transfection methods. Genet Eng Biotechnol News 27:4–6.

Du Y, Hu XH, Cariveau M, Ma X, Kalmus GW, Lu JQ. 2001. Optical properties of porcine skin dermis between 900 nm and 1500 nm. Phys Med Biol 46:167–181.

Feril JLB, Ogawa R, Kobayashi H, Kikuchi H, Kondo T. 2005. Ultrasound enhances liposome-mediated gene transfection. Ultrason Sonochem 12:489–493.

Hamm A, Krott N, Breibach I, Blindt R, Bosserhoff AK. 2002. Efficient transfection method for primary cells. Tissue Eng 8:235–245.

Harrison CA, Gossiel F, Layton CM, Bullock AJ, Johnson T, Blumsohn A, MacNeil S. 2006. Use of an in vitro model of tissue-engineered skin to investigate the mechanism of skin graft contraction. Tissue Eng 12:3119–3133.

Hearnden V, MacNeil S, Thornhill M, Murdoch C, Lewis A, Madsen J, Blanazs A, Armes S, Battaglia G. 2009. Diffusion studies of nanometer polymersomes across tissue engineered human oral mucosa. Pharm Res 26:1718–1728.

Hsiung PL, Nambiar PR, Fujimoto JG. 2005. Effect of tissue preservation on imaging using ultrahigh resolution optical coherence tomography. J Biomed Opt 10:064033.

Ishii K, Ma Z, Ninomiya Y, Takegoshi M, Kushibiki T, Yamamoto M, Hinds M, Tabata Y, Wang RK, Awazu K. 2007. Control of guided hard tissue regeneration using phosphorylated gelatin and OCT imaging of calcification. Prog Biomed Opt Imaging Proc SPIE 6439:64390D.

Kinikoglu B, Auxenfans C, Pierrillas P, Justin V, Breton P, Burillon C, Hasirci V, Damour O. 2009. Reconstruction of a full-thickness collagen-based human oral mucosal equivalent. Biomaterials 30:6418–6425.

Konig K, Riemann I. 2003. High-resolution multiphoton tomography of human skin with subcellular spatial resolution and picosecond time resolution. J Biomed Opt 8:432–439.

Kopchick JJ, Stacey DW. 1984. Differences in intracellular DNA ligation after microinjection and transfection. Mol Cell Biol 4:240–246.

Levitz D, Hinds MT, Wang RK, Zhenhe M, Ishii K, Tran N, McCarty OJT, Hanson SR, Jacques SL. 2007. A tissue-engineered 3D model of light scattering in atherosclerotic plaques. Prog Biomed Opt Imaging Proc SPIE 6439:643905.

Lomas H, Canton I, MacNeil S, Du J, Armes SP, Ryan AJ, Lewis AL, Battaglia G. 2007. Biomimetic pH sensitive polymersomes for efficient DNA encapsulation and delivery. Adv Mater 19:4238–4243.

Lomas H, Massignani M, Abdullah AK, Canton I, Lo Presti C, MacNeil S, Du J, Blanazs A, Madsen J, Armes S, Lewis AL, Battaglia G. 2008. Non-cytotoxic polymer vesicles for rapid and efficient intracellular delivery. Faraday Dis 139:143–159.

Martinet W, Schrijvers DM, Kockx MM. 2003. Nucleofection as an efficient nonviral transfection method for human monocytic cells. Biotechnol Lett 25:1025–1029.

Nehal KS, Gareau D, Rajadhyaksha M. 2008. Skin imaging with reflectance confocal microscopy. Semin Cutan Med Surg 27:37–43.

Rimmer S, Johnson C, Zhao B, Collier J, Gilmore L, Sabnis S, Wyman P, Sammon C, Fullwood NJ, MacNeil S. 2007. Epithelialization of hydrogels achieved by amine functionalization and co-culture with stromal cells. Biomaterials 28:5319–5331.

Schenke-Layland K. 2008. Non-invasive multiphoton imaging of extracellular matrix structures. J Biophoton 1:451–462.

Smith AM, Ruan G, Rhyner MN, Nie S. 2006. Engineering luminescent quantum dots for in vivo molecular and cellular imaging. Ann Biomed Eng 34:3–14.

Spöler F, Forst M, Marquardt Y, Hoeller D, Kurz H, Merk H, et al. 2006. High-resolution optical coherence tomography as a non-destructive monitoring tool for the engineering of skin equivalents. Skin Res Technol 12:261–267.

Studer D, Humbel BM, Chiquet M. 2008. Electron microscopy of high pressure frozen samples: Bridging the gap between cellular ultrastructure and atomic resolution. Histochem Cell Biol 130: 877–889.

Sun T, Haycock J, Macneil S. 2006. In situ image analysis of interactions between normal human keratinocytes and fibroblasts cultured in three-dimensional fibrin gels. Biomaterials 27:3459–3465.

Sun T, Norton D, Ryan AJ, MacNeil S, Haycock JW. 2007a. Investigation of fibroblast and keratinocyte cell-scaffold interactions using a novel 3D cell culture system. J Mater Sci Mater Med 18: 321–328.

Sun Y, Collett J, Fullwood NJ, MacNeil S, Rimmer S. 2007b. Culture of dermal fibroblasts and protein adsorption on block conetworks of poly(butyl methacrylate-block-(2,3 propandiol-1-methacrylate-stat-ethandiol dimethacrylate)). Biomaterials 28:661–670.

Sun Y, Tan HY, Lin SJ, Lee HS, Lin TY, Jee SH, Young TH, Lo W, Chen WL, Dong CY. 2008. Imaging tissue engineering scaffolds using multiphoton microscopy. Microsc Res Tech 71:140–145.

Tan W, Desai TA, Leckband D, Boppart SA. 2005. Optical coherence tomography of cell dynamics in three-dimensional engineered tissues. Prog Biomed Opt Imaging Proc SPIE 5699:102–110.

Tan W, Oldenburg AL, Norman JJ, Desai TA, Boppart SA. 2006. Optical coherence tomography of cell dynamics in three-dimensional tissue models. Opt Express 14:7159–7171.

White NS, Errington RJ. 2005. Fluorescence techniques for drug delivery research: Theory and practice. Adv Drug Deliv Rev 57: 17–42.

Yang Y, Dubois A, Qin XP, Li J, Haj AE, Wang RK. 2006a. Investigation of optical coherence tomography as an imaging modality in tissue engineering. Phys Med Biol 51:1649–1659.

Yang Y, Hoban PR, Sule-Suso J, Holley S, El Haj AJ, Bahrami F, Wang RK. 2006b. Study cell invasion by optical techniques. Proc SPIE 6084:60841A.

Yang Y, Bagnaninchi PO, Cunha-Reis C, Aydin HM, Piskin E, El Haj A. 2007. Characterisation of scaffold architecture by optical coherence tomography.

Yeh AT, Kao B, Jung WG, Chen Z, Nelson JS, Tromberg BJ. 2004. Imaging wound healing using optical coherence tomography and multiphoton microscopy in an in vitro skin-equivalent tissue model. J Biomed Opt 9:248–253.